2.A.1 *Nuclear Physics* **A128** (1969) 325–332; © *North-Holland Publishing Co., Amsterdam*

THE ^{3}He(α, γ)^{7}Be REACTION AT VERY LOW ENERGY

K. NAGATANI †, M. R. DWARAKANATH †† and D. ASHERY
California Institute of Technology, Pasadena, California †††

Received 17 February 1969

Abstract: Absolute cross sections for the ^{3}He(α, γ)^{7}Be reaction were determined for c.m. energies between 164 and 245 keV. The results are in good agreement with previous values obtained by Parker and Kavanagh, where the experiments overlap. The energy region was extended to lower energies and the accuracy of the measurement was improved.

E NUCLEAR REACTION ^{3}He(α, γ)^{7}Be, $E_{c.m.}$ = 164–245 keV; measured $\sigma(E)$. Enriched target.

1. Introduction

The direct capture reaction ^{3}He(α, γ)^{7}Be is of special interest in that it allows the study of a nonresonant capture mechanism over a wide energy range. This reaction is also of great interest in astrophysics, since it is involved in one of the terminating branches of the proton-proton chain. Parker and Kavanagh [1]) carried out an experimental investigation over a wide incident energy range (0.42 to 5.80 MeV in alpha bombarding energies). Tombrello and Parker [2]) accordingly made a theoretical analysis using known elastic scattering parameters. Their theoretical results agreed with the experimental data and permitted a confident extrapolation of the cross sections down to the energy region of astrophysical interest.

Recently there has been a renewed interest in the proton-proton chain. Davis, Harmer and Hoffman [3]) attempted a direct measurement of the solar neutrino flux, and Bahcall, Bahcall and Shaviv [4]) made a theoretical estimate of the counting rate based on the most recent nuclear reaction and solar model data. The upper limit obtained by Davis *et al.* was found to be somewhat lower than expected theoretically, but it appears that at the present state there is no irreconcilable discrepancy with the prediction when the uncertainties in the various parameters are taken into account. However, in order to interpret future measurements of the neutrino flux, the reaction data pertaining to the proton-proton chain should be carefully re-examined for possible errors in the extrapolation procedure. It is realized that the present reaction plays an especially important role in the mechanism, since the measurement of Davis *et al.*

† Now at Brookhaven National Laboratory, Upton, Long Island, New York.
†† Now at The Bhabha Atomic Research Centre, Bombay, India.
††† Supported in part by the National Science Foundation [GP–9114] and the Office of Naval Research [Nonr–220(47)].

has its largest sensitivity for the neutrinos from the ^{8}B decay, which is formed by the sequence ^{3}He(α, γ)^{7}Be(p, γ)^{8}B. In fact, Bahcall, Bahcall and Ulrich [5]) have shown that the counting rate in the ^{37}Cl neutrino flux experiment of Davis *et al.* depends on $S(0)^{0.8}$ where $S(0)$ in the low-energy cross-section factor for the ^{3}He(α, γ)^{7}Be reaction. It was, therefore, considered to be important to perform an independent experimental measurement of the absolute cross section of this reaction at very low energies with improved accuracy.

Direct measurement of the gamma rays was carried out to obtain the absolute capture cross sections for c.m. energies between 164 and 245 keV.

2. Procedure

A ^{4}He$^+$ ion beam was obtained from the Kellogg Radiation Laboratory 600 kV electrostatic generator. The alpha beam was used instead of a ^{3}He beam to minimize the gamma-ray background. The beam was analysed by magnetic deflection through 90°, giving a beam energy uncertainty of less than ± 2 % for beams of a few μA. A differentially-pumped, recirculating ^{3}He gas target system built by Dwarakanath and Winkler and described by Harrison *et al.* [6]) was employed. This technique eliminated a large uncertainty [1]) that would have arisen from the energy loss if an entrance foil had been used. Two high impedance gas canals were used in the system to maintain high vacuum (10^{-6} torr) in the accelerator tube and reasonable pressure in the target chamber. The analysed beam was passed through the first canal (10 cm long and 3.5 mm diameter) which allowed pressure of 10^{-2} torr for the intermediate pumping stage. The second canal (1.3 cm long and 3.5 mm diameter) was placed between the intermediate stage and the target entrance, giving a target pressure of up to 25 torr. The beam was collimated in front of the second canal by an aperture slightly smaller than the canal diameter. Recirculation of the ^{3}He gas was achieved by utilizing two Roots pumps (Heraeus Model R–1600 and Heraeus Model R–152). The gas was cleaned during recirculation by passing it through a zeolite absorber maintained at liquid nitrogen temperature, and fed back to the target chamber. The purity of the ^{3}He gas was estimated to be better than 99 %. The pressure of the gas was continuously monitored using an aneroid pressure gauge (Wallace and Tiernan) whose estimated accuracy was better than ± 2.5 % at the pressure used (15 torr). The pressure inside the second canal was calculated from the flow rate and using standard thermodynamic considerations; this gave an estimate that it was 58 % of the target chamber pressure. The temperature of the gas was measured at the target chamber wall. The local temperature in the beam was estimated [1]) to have negligibly small effect on the results.

The target chamber was made of a standard 5 cm aluminum pipe. At the end of the chamber, a calorimetric beam integrator [6, 7]) was placed to stop the beam and measure its intensity. It consists of two identical copper cups, one of which is heated by the beam while a compensating current is fed to a heater in the other cup. The two

cups contain matched thermistors as sensing elements serving as two arms of a bridge circuit. This device was previously calibrated and its accuracy was estimated to be better than $\pm 6\,\%$. This method avoids errors due to the unknown charge state of the beam at the end of the target. The target length was 9.5 cm from the end of the second canal to the integrator cup. The diameter of the beam was defined by the slit described earlier. The beam spread along the target due to multiple scattering was calculated to be negligibly small.

Since the cross section depends very strongly on the incident energy, the yield along the beam path changes rapidly as the beam loses energy. The energy loss was calculated using Whaling's [8]) tables with an accuracy of $\pm 10\,\%$. A typical energy loss through the whole length of the target was approximately 80 keV in lab energy. The energy straggling was also considered in the analysis. For the pressures and energies used, this amounted typically to a few keV.

A 7.6×7.6 cm NaI(Tl) crystal was used to detect the gamma rays. More than 10 cm thick lead shielding surrounded the side of the crystal. The detector was placed with its axis at 90° to the beam, and at 7.5 cm from the end of the second canal. At this particular position, the counting rate in the detector is estimated to be the maximum, when the yield and the efficiency along the target path are considered. The gamma-ray yield was determined by counting the area under the full energy peak. The conversion of this yield into an absolute cross section required an accurate knowledge of the photopeak efficiency along the target axis. Since the photopeak efficiency of such geometries cannot be easily calculated, it was experimentally measured by using calibrated point gamma-ray sources. The gamma-ray energies of primary interest were in the region between 1.84 and 1.75 MeV for the ground-state transitions ($^{3}He + \alpha$ lies 1.587 MeV above the ^{7}Be ground state). The gamma-ray sources used were two sets of ^{88}Y and ^{22}Na supplied by the Radiochemical Centre, England, and Commissariat à l'Energie Atomique, France (specified $\pm 2\,\%$ standard deviations). The intensities of those sources were re-examined by several independent methods: (1) comparing with other standard sources, (2) using the standard efficiency [9]) values of standard geometry, (3) comparison with another NaI(Tl) spectrometer in this laboratory [10]) whose efficiency calibration had been previously established directly by observing gamma rays from reactions such as $^{23}Na(p, \alpha\gamma)^{20}Ne$ etc. in which coincidences with charged particles were required. After these examinations, it was established that the intensity of the ^{88}Y source used was accurate to within $\pm 5\,\%$ and the ^{22}Na source used was accurate to within $\pm 10\,\%$. Once those intensities were determined, the photopeak efficiency was found as a function of energy and position along the target axis including the second canal section. Care was also taken to estimate the counts under the full energy peak, namely the background subtractions and sum peak corrections were standardized in these calibrations and in the actual runs. The inaccuracy of the final efficiency was estimated to be $\pm 5\,\%$ for the energy region of interest. Since this region is very close to the 1.836 keV ^{88}Y line, the $10\,\%$ inaccuracy in the Na source strength did not affect the result very much.

The gamma ray background was taken under two different situations; (i) without the beam, (ii) with the beam on ^{4}He gas in the target chamber. It was found that there were no noticeable differences in those two kinds of background. During the actual runs, background measurements were repeated and no change was observed. By taking a background run over a sufficiently long time, the statistical error in the background spectrum was reduced.

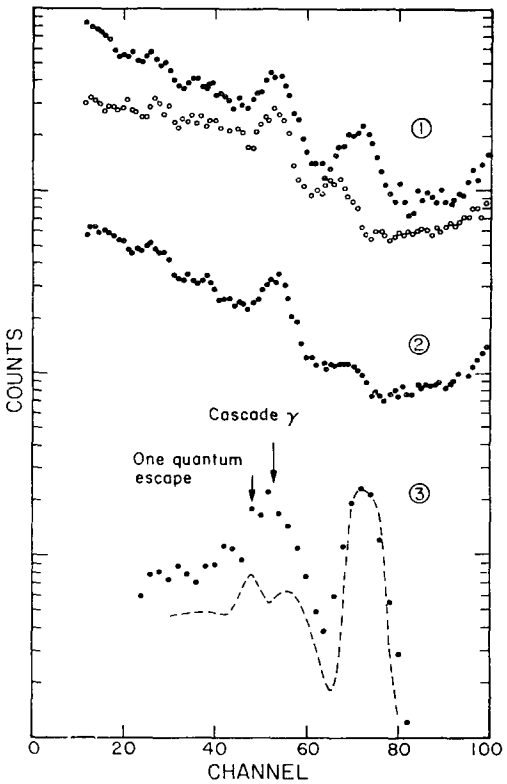

Fig. 1. Gamma ray spectra: The solid points in 1 for the spectrum are taken at an incident energy of 614 keV, and the open circles in 1 for the spectrum are taken at incident energy of 418 keV. The spectrum 2 is a background spectrum. Points in 3 indicate the net spectrum at the incident energy of 614 keV. The dashed curve in 3 represents the 1.836 ^{88}Y gamma-ray spectrum shape. The normalizations are arbitrary.

In fig. 1, a background spectrum is displayed by the spectrum 2. The peak centered at channel 53 corresponds to the 1.46 MeV gamma ray from ^{40}K present in the surrounding materials. The rise in the higher energy channels was believed to be the tail from high-energy gamma rays from heavy elements present in the lead shielding, and, possibly, from cosmic rays.

In the actual measurement, seven runs were carried out with the incident energies of 418, 454, 505, 515, 566, 570, and 614 keV. The gamma-ray spectrum of the 614 keV

incident energy run is shown in fig. 1 (labeled 1, solid points). The open circles in the spectrum show the spectrum shape for the incident energy of 418 keV (the relative normalization given here is arbitrary). Spectrum 3 shows the net spectrum after background has been subtracted for the 614 keV run (again the normalization is arbitrary). In order to extract the cascade gamma rays, the spectrum shape of the 1.836 MeV gamma ray from the ^{88}Y source measured in the same geometry was used, shown by the dashed curve in the spectrum 3 of fig. 1. It is noticed that the 1.83 MeV (ground-state transition gamma ray) peak is wider than the ^{88}Y spectrum. This is due to the energy spread in the reaction gamma ray because of the energy loss along the target path. There are obviously net counts at the cascade gamma-ray energy, although the shape is not clear. The number of counts for the cascade gamma ray was, therefore, estimated by taking the net counts in the proper channels. This process was possible for three of the seven runs, i.e., those of the incident energies of 505, 566, and 614 keV. The branching ratios obtained were in agreement with those measured at higher bombarding energies [1]) as shown in fig. 4; accordingly Parker's more accurate value of $\rho = 0.374 \pm 0.056$ was used to determine the total cross sections. The theoretical values for the angular distribution coefficients calculated in ref. [2]) were also used in the reduction of the data; the corrections amount to 3 %. Corrections for the sum peaks due to the cascade transitions – amounting to 3 % – were also made.

3. Results and discussion

In the present experiment, the gamma-ray yield can be written as

$$Y = \int_0^L \frac{\mathrm{d}Y}{\mathrm{d}l}\,\mathrm{d}l,$$

where Y and $\mathrm{d}Y/\mathrm{d}l$ are the total yield and yield per unit length of target at the position given by l, and L is the total target length.

$$\frac{\mathrm{d}Y}{\mathrm{d}l} = a\sigma(E)N_\mathrm{i}N_\mathrm{t}(l)\mathscr{E}(E, l),$$

where a is the angular distribution factor which is obtained from the crystal-target geometry and the theoretical angular distribution coefficients [2]), N_i and $N_\mathrm{t}(l)$ are the number of incident α-particles and the density of target nuclei (^{3}He) at position l. The latter depends on the position l only in the neighborhood of the canal where the density is changing. $\mathscr{E}(E, l)$ is the detection efficiency, $\sigma(E)$ is the reaction cross section at energy E (the energy E depends on l) and $\sigma(E)$ can be written as

$$\sigma(E) = S(E)\frac{\exp(-2\pi\eta)}{E}, \quad \text{where } \eta = \frac{Z_1 Z_2 e^2}{\hbar v}.$$

Here $S(E)$ is the familiar cross section factor [11]) which is the reaction cross section with the explicit energy dependence factored out. It is essentially a constant in the

energy interval over which the yields are obtained. Thus $S(E)$ is brought outside the integration and set equal to $S(E_0)$ where E_0 is the mean c.m. energy defined by

$$E_0 = \frac{1}{Y}\int_0^L E\frac{\mathrm{d}Y}{\mathrm{d}l}\,\mathrm{d}l.$$

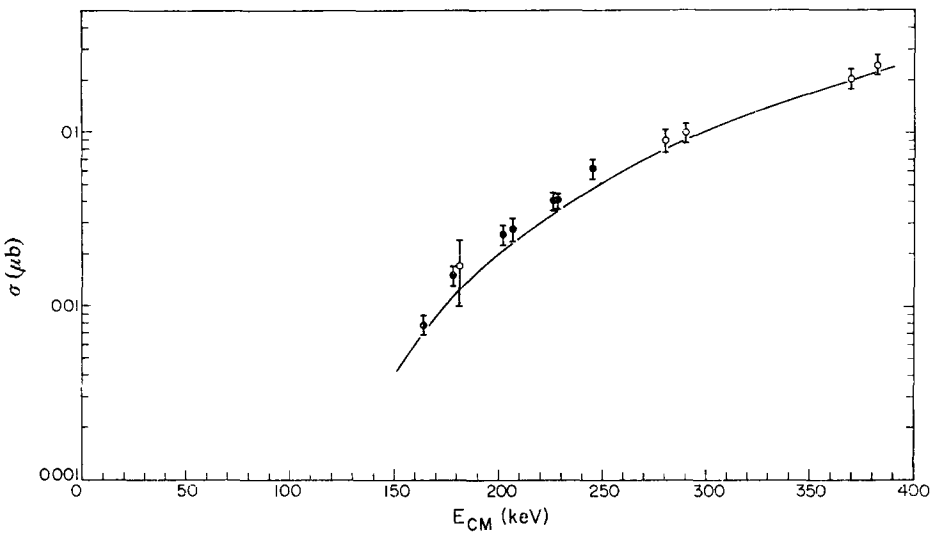

Fig. 2. The cross sections $\sigma(E)$: The solid points are the present results while the open circles are those of Parker's corrected values [12]). The solid curve indicates the theoretical prediction of ref. [2]).

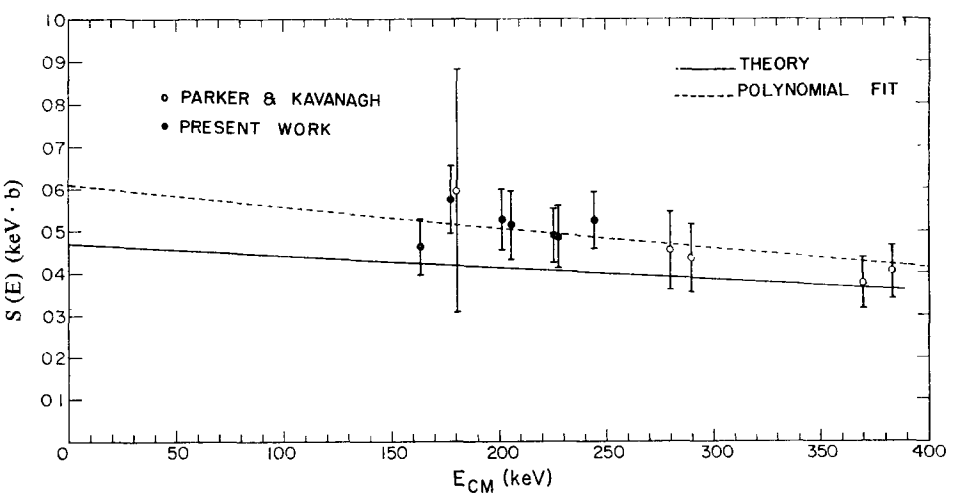

Fig. 3. The cross-section factor $S(E)$: The solid points are the present results while the open circles are those of Parker's corrected values [12]). The solid curve indicates the theoretical prediction of ref. [2]), while the dashed curve shows the result of the least squares polynomial fit.

For energy E expressed in keV, the yield is given by

$$Y = aN_i S(E_0) \int_0^L \frac{1}{E} \exp(-163 \cdot 78/\sqrt{E}) \mathscr{E}(E, l) N_t(l) \mathrm{d}l.$$

The integration is performed numerically to obtain $S(E_0)$ from the measured quantities. The errors discussed earlier are combined with the statistical errors (always under $\pm 12\%$) to obtain the total uncertainty in $S(E_0)$. The uncertainty in $S(E_0)$ is $\pm 15\%$ at the lowest energy where the cross section is very small and the counting

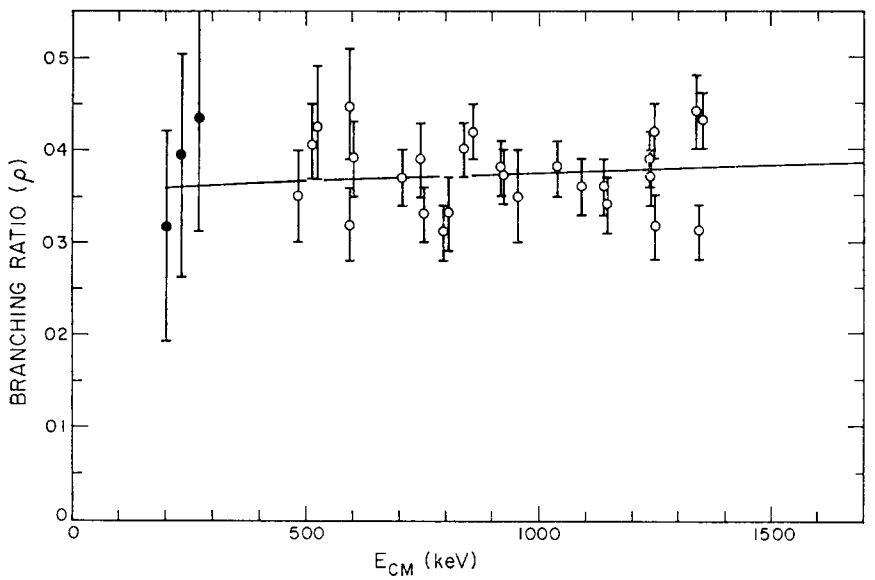

Fig. 4. The branching ratios ρ: The solid points are the present results while the open circles are those in ref. [1]). The solid curve indicates the theoretical prediction of ref. [2]).

statistics poor. Figs. 2–4 show the present results together with the results of Parker and Kavanagh obtained previously †. The theoretical results of Tombrello and Parker are shown by solid lines. The dashed line in fig. 3 represents a polynomial least-squares fit to the data obtained in the present work plus that by Parker and Kavanagh up to 800 keV in the c.m.

As illustrated, the present results are in excellent agreement with the previous ones. However, having now more data available in the low-energy region, and with improved accuracy, it can be noted more positively than before that all the experimental values are higher than the theoretical calculations. A second order (in energy) polynomial fit to the data gives the value of $S(0) = 0.61 \pm 0.07$ keV · b and $(\mathrm{d}S/\mathrm{d}E)_0 =$

† During the course of this work, Dr. P. D. Parker [12]) noticed that the error treatment in energy loss was made incorrectly in ref. [1]). It has been corrected and the results shown in figs. 2 and 3 are the correct results.

$-(5.8\pm0.3)10^{-4}$ b (fig. 3). The theoretical curve shown in fig. 3 was obtained using an overall normalization to all the experimental values obtained in the present work and by Parker and Kavanagh. If the normalization is done taking the data only from the low-energy region (up to 700 keV in the c.m.), the theoretical curve is shifted up and yields the values $S(0) = 0.51\pm0.05$ keV · b and $(\mathrm{d}S/\mathrm{d}E)_0 = -(2.8\pm0.4)10^{-4}$ b. The previous theoretical curve [1,2]) adjusted to all the data up to 2500 keV yielded $S(0) = 0.47\pm0.05$ keV · b and $(\mathrm{d}S/\mathrm{d}E)_0 = -(2.8\pm0.4)10^{-4}$ b. It should be noted, however, that although the theoretical calculations taken up to 700 keV, and the polynomial fit agree, within the errors, in the value of $S(0)$, there still exists a clear inconsistency between the two in the value of the slope. The implication of these results on the solar neutrino experiment [3]) is that, using the dependence of the counting rate on $[S_{34}(0)]^{0.8}$ (ref. [5])) the predicted counting rate is increased by 10 % or 23 % [over the values computed using Parker's $S(0)$], depending on whether the theoretical or the polynomial fit, respectively, is used.

The authors wish to thank Professors J. N. Bahcall, William A. Fowler and T. A. Tombrello for suggesting this experiment and for their helpful discussions.

References

1) P. D. Parker and R. W. Kavanagh, Phys. Rev. **131** (1963) 2578
2) T. A. Tombrello and P. D. Parker, Phys. Rev. **131** (1963) 2582
3) R. Davis, Jr., D. S. Harmer and K. C. Hoffman, Phys. Rev. Lett. **20** (1968) 1205
4) J. N. Bahcall, N. A. Bahcall and G. Shaviv, Phys. Rev. Lett. **20** (1968) 1209
5) J. N. Bahcall, N. A. Bahcall and R. K. Ulrich, to be published in Astrophys. J. (May 1969)
6) W. D. Harrison, W. E. Stephens, T. A. Tombrello and H. Winkler, Phys. Rev. **160** (1967) 752
7) M. R. Dwarakanath and H. Winkler, Bull. Am. Phys. Soc. **12** (1967) 16
8) W. Whaling, Handbuch der Physik **34** (1958) 193
9) R. L. Heath, Scintillation Spectroscopy I, IDD–16880–1 Research and development report, TID–4500 (1964) Appendix III
10) P. B. Lyons, J. W. Toevs and D. G. Sargood, to be published
11) E. M. Burbidge, G. R. Burbidge, W. A. Fowler and F. Hoyle, Rev. Mod. Phys. **29** (1957) 547
12) P. D. Parker, private communication